

## **A NOVEL SYNTHESIS TECHNIQUE FOR MICROWAVE BANDPASS FILTERS WITH FREQUENCY-DEPENDENT COUPLINGS**

**Natalia Leszczynska<sup>\*</sup>, Lukasz Szydowski,  
and Michal Mrozowski**

Faculty of Electronics, Telecommunications and Informatics, Gdansk University of Technology, 11/12, G. Narutowicza St., Gdansk 80-233, Poland

**Abstract**—This paper presents a novel synthesis technique for microwave bandpass filters with frequency-dependent couplings. The proposed method is based on the systematic extraction of a dispersive coupling coefficient using an optimization technique based on the zeros and poles of scattering parameters representing two coupled resonators. The application of this method of synthesis is illustrated using two examples involving four and five-pole generalized Chebyshev filters implemented in substrate-integrated waveguide (SIW) technology. As a dispersive inverter, a parallel shorted stub with an additional septum was used. The septum lends greater flexibility to the dimensional synthesis, in that it increases the allowable range of the coupling coefficients. The measured and simulated results are in excellent agreement, which confirms the validity of the proposed approach.

### **1. INTRODUCTION**

The increase in the capacity and complexity of modern terrestrial and satellite communications systems has led to a need for filters with sharp cut-off characteristics and high out-of-band rejection. To meet these requirements, filters exhibiting quasielliptic responses [1, 2] are most commonly used. Classical design methods [3–5] synthesize such responses using coupled-cavity filter topologies with constant direct and cross-couplings between the resonators. However, aiming for high selectivity, synthesis often results in coupling schemes that may be difficult to implement.

---

*Received 10 January 2013, Accepted 30 January 2013, Scheduled 7 February 2013*

\* Corresponding author: Natalia Leszczynska (leszczynska.natalia@gmail.com).

On the other hand, using cross-coupled resonators is not the only way to introduce transmission zeros (TZs) into the filter characteristics. In the last decade, it has been demonstrated that even directly coupled resonators may exhibit responses with TZs if frequency-dependent couplings are used [6,7]. In particular, such couplings allow the synthesis of quasielliptic responses in in-line topologies, assuring sharp cut-off skirts with symmetric and asymmetric responses. However, one of the main obstacles hindering the widespread application of such filters is a lack of accurate synthesis techniques. In fact, almost all successful designs of such filters have been achieved by extensive full-wave optimization. This approach is very time consuming, even if surrogate models [8] or GPU-accelerated solvers [9–12] are used. On the other hand, an in-line topology is the simplest topology, and it is well known that all-pole filters can be synthesized very accurately using, e.g., Cohn's synthesis [13]. An in-line arrangement of resonators is very favorable, as such filters are easy to implement. It is hence desirable to develop an accurate synthesis technique which is also valid for in-line filters with quasielliptic responses implemented using dispersive inverters.

In this paper, we propose a novel synthesis technique for generalized Chebyshev filters with frequency-dependent couplings. The method is an improved version of a technique developed recently in our group, presented in [14]. In its original version, the synthesis matches the scattering parameters of two coupled resonators with those resulting from a coupling submatrix, assuming the frequency-dependent coefficient. However, this method does not account for the loading effect that results from the other resonators present in the filter. As a result, the design is always detuned. The new method matches the zeros and poles of the scattering parameters representing two coupled resonators. To obtain the reference zeros and poles, a submatrix representing the electrical behavior of two coupled resonators is extracted from the final coupling matrix by deleting appropriate rows and columns. Next, the values of the external couplings in the submatrix are recalculated to take into account the loading effect. We demonstrate the synthesis procedure with two examples. The chosen examples involve four and five-pole in-line pseudoelliptic generalized Chebyshev filters with two transmission zeros implemented in SIW (substrate-integrated waveguide) technology. Direct couplings are realized as inductive irises, while the dispersive couplings are implemented via a shorted stub with an additional septum placed perpendicularly or in parallel to the direction of propagation.

Substrate-integrated waveguide SIW technology [15–18] offers easy fabrication, higher-quality factors than other planar circuits,

repeatability, and a relatively low cost of production. Since SIW operates as a rectangular waveguide, the easiest way of introducing dispersive couplings is by means of shorted stubs. Examples of in-line SIW filters with stubs may be found in the literature [19]. However, a simple parallel shorted stub allows for transmission zeros near the filter band, which limits the range of allowable responses. A modified stub was shown in [14], where an additional septum was introduced to locate the TZ farther from the passband. The parallel septum considered in one of our examples has not been proposed in the literature to date. The septa in the stubs are essential for obtaining better control over the location of the transmission zeros.

## 2. SYNTHESIS

Before describing the method of synthesis, we recall some fundamental formulations concerning filter design. Figure 1 presents a general model of multiple coupled resonators in the prototype domain. The impedance matrix of the proposed model has the following form

$$\mathbf{Z} = \mathbf{M}_0 + \omega\mathbf{M}_1 - j\mathbf{R} \tag{1}$$

where  $\mathbf{M}_0, \mathbf{M}_1$  are  $(N + 2, N + 2)$  matrices. In the classical approach, when the couplings are frequency-independent,  $\mathbf{M}_1$  is the identity matrix. Introducing off-diagonal elements to  $\mathbf{M}_1$ , we obtain the impedance matrix of a filter with dispersive couplings [20]. In this case, the matrices  $\mathbf{M}_0$  and  $\mathbf{M}_1$  are responsible for the constant and dispersive part of the coupling coefficients, respectively. In Eq. (1),  $\mathbf{R}$  is an  $(N + 2, N + 2)$  terminating matrix with all elements equal to zero, except for  $R(1, 1) = R(N + 2, N + 2) = 1$ , while  $\omega$  denotes the prototype angular frequency. The scattering parameters of a two-port network

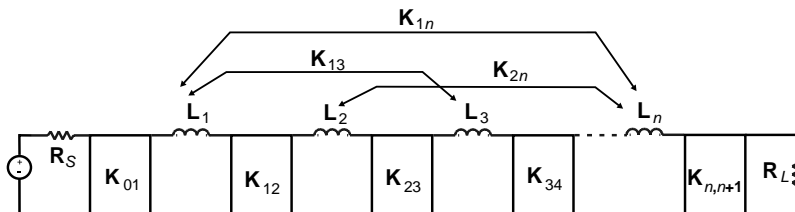


**Figure 1.** General model of a multiply coupled resonator bandpass filter.

are related to the impedance matrix via the following equations [20]:

$$S_{11} = \frac{F}{E} = -1 - 2j \frac{\det(\mathbf{M}'_0 + \omega \mathbf{M}'_1 - j \mathbf{R}')}{\det(\mathbf{M}_0 + \omega \mathbf{M}_1 - j \mathbf{R})} \quad (2)$$

$$S_{21} = \frac{P}{\varepsilon E} = 2j \frac{\det(\mathbf{M}''_0 + \omega \mathbf{M}''_1 - j \mathbf{R}'')}{\det(\mathbf{M}_0 + \omega \mathbf{M}_1 - j \mathbf{R})}. \quad (3)$$

where matrices  $\mathbf{M}'_0$ ,  $\mathbf{M}'_1$ ,  $\mathbf{R}'$ , are the upper principal submatrices obtained by deleting the last row and column of the matrices  $\mathbf{M}_0$ ,  $\mathbf{M}_1$  and  $\mathbf{R}$ , respectively. Matrices  $\mathbf{M}''_0$ ,  $\mathbf{M}''_1$ ,  $\mathbf{R}''$  are created in a similar fashion, except that this time the first row and the last column are deleted. From Eqs. (2)–(3) it can be seen that the common poles of  $S_{11}$  and  $S_{21}$  are generalized eigenvalues of a matrix pencil ( $[\mathbf{M}_0 - j \mathbf{R}_0]$ ,  $\mathbf{M}_1$ ), while the zeros of  $S_{21}$  are the generalized eigenvalues of a matrix pencil ( $[\mathbf{M}''_0 - j \mathbf{R}''_0]$ ,  $\mathbf{M}''_1$ ), all multiplied by  $-j$ . Note that the zeros of  $S_{11}$  cannot be simply identified with a proper pencil; instead, Eq. (2) must be reformulated thus:

$$\frac{F + E}{E} = \frac{F'}{E} = -2j \frac{\det(\mathbf{M}'_0 + \omega \mathbf{M}'_1 - j \mathbf{R}')}{\det(\mathbf{M}_0 + \omega \mathbf{M}_1 - j \mathbf{R})}. \quad (4)$$

It can be seen from the above expression, that the roots of the new polynomial  $F'$  may be found as the generalized eigenvalues of a matrix pencil ( $[\mathbf{M}'_0 - j \mathbf{R}'_0]$ ,  $\mathbf{M}'_1$ ) and finally the zeros of  $S_{11}$  can be computed as the roots of the polynomial  $-E + 2F'$  (which equals  $F$ ). For a given quasielliptic filtering function, the constant and dispersive parts of the coupling matrix can be found using the procedure proposed in [20]. This step completes the process of extracting the zeros and poles of the scattering polynomials representing a two-port network.

On the other hand, the values of the coupling coefficients resulting from the prototype coupling matrix are related to the inverter values via the following equations [13]:

$$K_{S1} = \sqrt{\alpha_1 FBW R_S} \cdot m_0^{S1} \quad (5)$$

$$K_{NL} = \sqrt{\alpha_N FBW R_L} \cdot m_0^{NL} \quad (6)$$

$$K_{i,j} = FBW \sqrt{\alpha_i \alpha_j} \cdot \left( m_0^{i,j} + \omega m_1^{i,j} \right) \quad (7)$$

$$\alpha_j = \frac{\omega_0}{2} \left. \frac{dX_j(\omega)}{d\omega} \right|_{\omega=\omega_0} \quad (8)$$

$$FBW = \frac{\omega_2 - \omega_1}{\omega_0} \quad (9)$$

where  $K_{S1}$ ,  $K_{NL}$ ,  $K_{i,j}$  denote the denormalized values of inverters representing the couplings from source to the first resonator, from the last resonator to load, and between resonators, respectively. FBW is

the fractional bandwidth where  $\omega_2$ ,  $\omega_1$ ,  $\omega_0$  denote the band edge and center angular frequencies, respectively. The slope parameter of an  $i$ -th resonator  $\alpha_i$  is given as a first derivative of the reactance of the resonator multiplied by half of the resonant frequency. It can be clearly seen that the external couplings are scaled in a different manner than are the internal couplings. This observation is important, and will be exploited later in the synthesis.

Once the coupling matrix of the filter has been found using the procedure described in [20], the dimensional synthesis can begin. To this end, we have recently proposed a method [14] involving frequency-dependent inverter, based on the extraction of the coupling submatrix of coupled resonators with the assumption that external couplings are sufficiently small to avoid any frequency shift. Next, the designer performs dimensional synthesis based on tuning the geometrical parameters to match the scattering parameters obtained from the numerical simulation with those resulting from the extracted submatrix. Such an approach gives relatively good results, but does suffer from the assumption that the external couplings are relatively small. This assumption leads to the detuning of the resonators, since the loading effect due to the other resonators present in the filter is omitted. This issue can be overcome when the true values of the external inverters are taken into account. Let us consider an in-line filter of an arbitrary order  $N$  with a frequency-dependent coupling placed between the first and the second resonator. The overall impedance matrix has the following form

$$\mathbf{Z} = \begin{bmatrix} -j & m_0^{S1} & 0 & 0 & 0 & 0 \\ m_0^{S1} & m_0^{11} + \omega & m_0^{12} + \omega m_1^{12} & 0 & \dots & 0 \\ 0 & m_0^{12} + \omega m_1^{12} & m_0^{22} + \omega & m_0^{23} & \vdots & 0 \\ 0 & 0 & m_0^{23} & \ddots & & 0 \\ 0 & \vdots & 0 & & m_0^{NN} + \omega & m_0^{NL} \\ 0 & 0 & 0 & 0 & m_0^{NL} & -j \end{bmatrix}.$$

Now, to extract the impedance submatrix  $\mathbf{Z}^{12}$  describing the electrical behavior of two resonators coupled through the frequency-dependent inverter, all rows and columns from the fifth to the last must be removed. This results in the following matrix

$$\mathbf{Z}^{12} = \begin{bmatrix} -j & m_0^{S1} & 0 & 0 \\ m_0^{S1} & m_0^{11} + \omega & m_0^{12} + \omega m_1^{12} & 0 \\ 0 & m_0^{12} + \omega m_1^{12} & m_0^{22} + \omega & m_0^{23} \\ 0 & 0 & m_0^{23} & -j \end{bmatrix}.$$

Referring to the technique presented in [14], at this stage of our

previous synthesis procedure,  $m_0^{S1}$  and  $m_0^{23}$  should be set to small values such as 0.02. However, as explained above, this will cause the loading effect to become negligible, affecting the overall filter response. To overcome this, the values resulting from the impedance submatrix  $\mathbf{Z}^{12}$  cannot be used as is. This follows directly from Formulas (5)–(7). Since the value of the denormalized external coupling seen by the load must be equal to the denormalized value of the internal coupling,  $m_0^{23}$  must be recalculated using the following formula:

$$m_0^{23'} = \frac{\sqrt{\alpha_2 \alpha_3} FBW}{\sqrt{\alpha_2 FBW R_L}} m_0^{23}. \quad (10)$$

This should then be substituted for  $m_0^{23}$  in the impedance matrix  $\mathbf{Z}^{12}$ . Setting  $R_l = Z_0$ , and assuming that the filter consists of half-wavelength resonators, we can evaluate the slope parameter [13]. In this case, Eq. (10) takes on the following form:

$$m_0^{23'} = \sqrt{\frac{\pi}{2} FBW_\lambda} \cdot m_0^{23} \quad (11)$$

where  $FBW_\lambda$  is the fractional bandwidth based on guided wavelengths. When the submatrix corresponding to two resonators coupled through a dispersive coupling is extracted and modified according to (11), we can proceed to the dimensional synthesis. Rather than matching the scattering parameters directly, we apply the zero-pole technique proposed in [21] adapted for a single coupling. In this new variant, the reference poles for a pair of resonators are evaluated by solving the generalized eigenvalue problems, formulated for polynomials of  $S_{11}$  and  $S_{21}$  (see Eqs. (2)–(3)) where  $M_0$  and  $M_1$  are  $4 \times 4$  coupling submatrices obtained using the procedure outlined above. With the reference zeros and poles extracted from the new impedance submatrix, the dimensional synthesis problem may be formulated as an optimization routine with the following error function

$$\Delta E = (\lambda_0 - \lambda)^H (\lambda_0 - \lambda) \quad (12)$$

where  $\lambda_0$  is a reference set of zeros and poles extracted as generalized eigenvalues from the target submatrix, and  $\lambda$  is a vector of the corresponding zeros and poles obtained at each iteration from the rational representation of the scattering parameter of the physical structure computed by a full-wave simulator. To obtain the rational model, a vector-fitting technique [22] can be used.

If multiple frequency-dependent couplings exist in the circuit, they can be synthesized in a similar way. However, it should be pointed out that coupled pairs of resonators need to be separated by at least one constant coupling. This restriction can be removed (e.g., by considering three cascaded resonators instead of two), but this will not be discussed in the present paper.

### 3. FILTER DESIGNS

To verify the method outlined in the previous section, two bandpass filters with quasielliptic characteristics have been designed. The filters have been fabricated on a Taconic RF-35 substrate, which has a relative dielectric constant equal to 3.47 and a thickness of 0.737 mm. A standard low-cost PCB process was used to manufacture both circuits. All metalized vias have the same diameter of 1 mm, and the spacing between their centers is equal to 1.5 mm.

#### 3.1. Fourth-order *E*-plane in-line SIW Filter

The first example of the technique outlined in the previous section is an in-line fourth-order generalized Chebyshev filter centered at  $f_0 = 5.395$  GHz, with bandwidth equal to 225 MHz. The filter has a 20 dB return loss and two transmission zeros located on either side of the passband at  $f_{z1} = 5.14$  GHz and  $f_{z2} = 5.747$  GHz. The filter is composed of four directly connected resonant cavities with frequency-dependent coupling placed between the first and the second resonator, and also between the third and the fourth. The external septa are offset from the center of the filter by three millimeters. To obtain the overall impedance matrix, the approach presented in [20] was used. For this particular case, it has the following form:

$$\mathbf{Z} = \begin{bmatrix} -j & 0.9411 & 0 & 0 & 0 & 0 \\ 0.9411 & 0.6866+\omega & 0.9440+0.4037\omega & 0 & 0 & 0 \\ 0 & 0.9440+0.4037\omega & 0.4180+\omega & 0.6284 & 0 & 0 \\ 0 & 0 & 0.6284 & -0.3446+\omega & -0.9321+0.3067\omega & 0 \\ 0 & 0 & 0 & -0.9321+0.3067\omega & -0.5475+\omega & 0.9791 \\ 0 & 0 & 0 & 0 & 0.9791 & -j \end{bmatrix}.$$

Next, the submatrices representing the resonators coupled through dispersive inverters must be extracted. First, the submatrix responsible for the coupled resonators 1 and 2 is considered. To obtain this, all rows and columns from the fifth to the sixth are deleted, resulting in:

$$\mathbf{Z}^{12} = \begin{bmatrix} 0 & 0.9411 & 0 & 0 \\ 0.9411 & 0.6866 + \omega & 0.9440 + 0.4037\omega & 0 \\ 0 & 0.9440 + 0.4037\omega & 0.4180 + \omega & 0.2121 \\ 0 & 0 & 0.2121 & 0 \end{bmatrix}.$$

Note that value of the constant coupling between resonators 2 and 3 was recalculated using the formula (11), yielding  $m'_{23} = 0.2121$ . The matrix representing coupled resonators 3 and 4 is obtained in a similar

way, except that this time the first two rows and columns are deleted from matrix  $\mathbf{Z}$ . After the renormalization of the external coupling according to (11), the submatrix becomes

$$\mathbf{Z}^{34} = \begin{bmatrix} 0 & 0.2121 & 0 & 0 \\ 0.2121 & -0.3446 + \omega & -0.9321 + 0.3067\omega & 0 \\ 0 & -0.9321 + 0.3067\omega & -0.5475 + \omega & 0.9791 \\ 0 & 0 & 0.9791 & 0 \end{bmatrix}.$$

With the impedance submatrices of the coupled resonators now determined, the reference zeros and poles may be extracted, by finding the eigenvalues of the generalized eigenproblems introduced above. For the first coupled pair, the reference values are as follows:

$$\begin{aligned} rE_{12} &= [-0.7286 + 0.5249j, -0.3833 - 0.9338j], \\ rF_{12} &= [-0.3585 - 0.9005j, -0.6459 + 0.4916j], \\ rP_{12} &= [-2.3382j] \end{aligned}$$

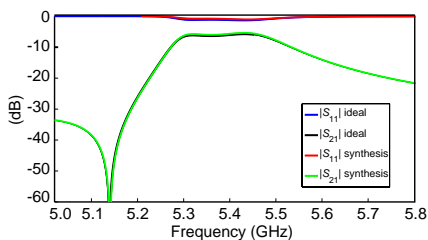
while for the second pair, they read

$$\begin{aligned} rE_{34} &= [-0.6872 - 0.5585j, -0.4207 + 0.9121j], \\ rF_{34} &= [0.3909 + 0.8790j, 0.6176 - 0.5254j], \\ rP_{34} &= [3.0392j]. \end{aligned}$$

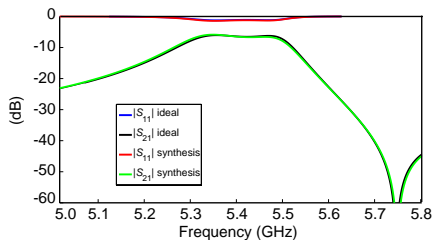
The final step is dimensional synthesis. In general, the direct couplings are implemented as inductive  $E$ -plane irises, while the frequency-dependent couplings can be implemented as shorted stubs. Such implementations are described well in the literature [19]. For this application, a shorted stub with a septum placed in parallel to the direction of propagation is employed. Such a modification makes the dimensional synthesis more flexible in terms of the allowable range of coupling coefficients, and to the best knowledge of the authors, has not been proposed to date.

Figures 2 and 3 show a comparison between the simulated and the ideal scattering parameters of the coupled pairs of resonators 1–2 and 3–4, respectively. Within a few iterations of a zero-pole algorithm [19], an almost perfect match was achieved. The initial filter response after assembling the synthesized pairs is presented in Figure 4. It can be observed that the transmission zeros are placed at the desired frequencies, and the filter band is as specified. The only discrepancy concerns the return loss level, which was degraded to approximately 11 dB from the assumed 20 dB. Such initial filter design is an excellent starting point for final tuning. For this particular case, only four iterations of the zero-pole procedure [21] were needed to complete the design. The filter layout and the corresponding dimensions are presented in Figure 6 and Table 1, respectively. Additionally, in order

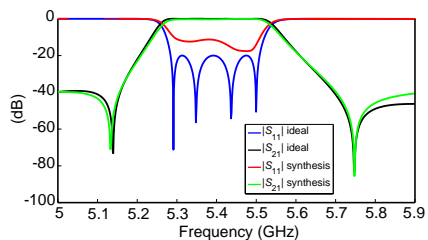




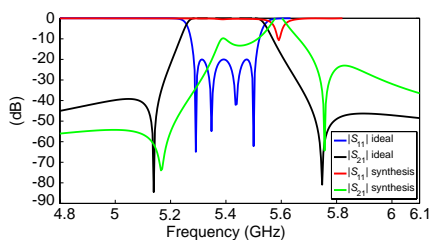
**Figure 2.** Synthesis of dispersive coupling between first and second resonators.



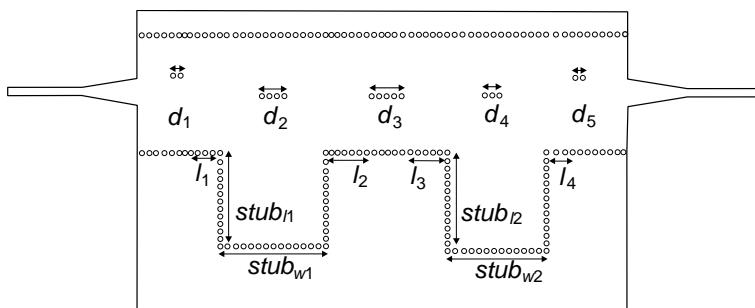
**Figure 3.** Synthesis of dispersive coupling between third and fourth resonators.



**Figure 4.** Comparison between the synthesized and the ideal filter response.



**Figure 5.** Comparison between the characteristics obtained with the synthesis shown in [14] and the ideal.

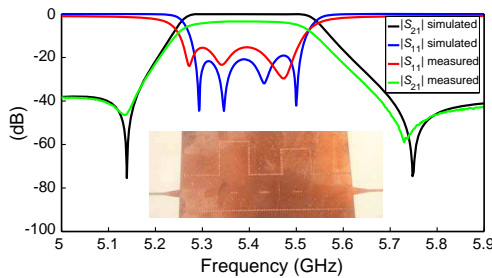


**Figure 6.** Layout of filter.

to show the potential and accuracy of the proposed technique, we have contrasted the results of the new synthesis technique with the results obtained using the method presented in [14]. Figure 5 shows a comparison between the assumed filter response and the response obtained after the synthesis performed according to [14]. As can

**Table 1.** Dimensions for the  $E$ -plane substrate-integrated waveguide filter with quasielliptic characteristics.

$Parameter$	$x_{synthesis}$	$x_{optimization}$	$Parameter$	$x_{synthesis}$	$x_{optimization}$
$l_1$	8.8546	8.1423	$d_4$	3.8100	3.1043
$l_2$	9.9955	9.3072	$d_5$	1.4569	1.4189
$l_3$	7.5460	7.0907	$stub_{l1}$	18.8640	17.6257
$l_4$	6.8906	6.3348	$stub_{l2}$	24.7285	23.3637
$d_1$	1.2461	1.3495	$stub_{w1}$	18.8330	19.5235
$d_2$	5.4225	4.7517	$stub_{w1}$	18.8330	19.5235
$d_3$	6.5209	5.7292			

**Figure 7.** Comparison of simulated and measured filter responses (the inset shows a photograph of the circuit).

be seen, only the positions of the transmission zeros are synthesized properly. It is also obvious that none of the specified parameters of the filter band are met. This implies that taking the loading effect into account is crucial for successful dimensional synthesis of the pair of coupled resonators.

A comparison between the measured component and the ideal characteristics is presented in Figure 7. As can be seen, the filter return loss performance has been degraded to approximately 15 dB, which is still a satisfactory result. This effect is mainly due to the imperfections of the fabrication process, which lead to detuning of the resonators. The transmission zeros are located almost at the desired frequencies, which ensures the assumed rejection level. The filter insertion loss level is around 3.4 dB, and is mainly the result of dielectric loss and poor metalization of the via-holes. Nevertheless, the measured characteristics are in good agreement with the simulated data. A photograph of the fabricated device is shown in the inset in Figure 7.

### 3.2. Fifth-order *H*-plane in-line SIW Filter Design

The second example is an in-line fifth-order filter centered at  $f_0 = 5.1$  GHz with bandwidth equal to 300 MHz. The filter has a 20 dB return loss and two transmission zeros located on the upper side of the passband at  $f_{z1} = 5.353$  GHz and  $f_{z2} = 5.49$  GHz. The filter consists of five directly connected resonator cavities with a frequency-dependent coupling placed between the first and second resonators and between fourth and fifth resonators, and is presented in Figure 8. In this example, the frequency-dependent coupling is realized as a shorted stub with vertical septum. As in the previous case, the septum allows better control over the position of the transmission zeros. Similarly to the previous case, the design starts with the synthesis of the coupling matrix. After a few iterations of the synthesis algorithm [20], the following impedance matrix was achieved

$$\mathbf{Z} = \begin{bmatrix} j & 0.8455 & 0 & 0 & 0 & 0 & 0 & 0 & 0 & 0 & 0 \\ 0.8455 & -0.8417+\omega & 0.9191-0.5527\omega & 0 & 0 & 0 & 0 & 0 & 0 & 0 & 0 \\ 0 & 0.9191-0.5527\omega & -0.4770+\omega & 0.5562 & 0 & 0 & 0 & 0 & 0 & 0 & 0 \\ 0 & 0 & 0.5562 & 0.1271+\omega & 0.6072 & 0 & 0 & 0 & 0 & 0 & 0 \\ 0 & 0 & 0 & 0.6072 & -0.2724+\omega & 0 & 0 & 0 & 0 & 0 & 0 \\ 0 & 0 & 0 & 0 & 0 & 0.8811-0.3486\omega & 0 & 0 & 0 & 0 & 0 \\ 0 & 0 & 0 & 0 & 0 & 0.8811-0.3486\omega & 0 & 0 & 0 & 0 & 0 \\ 0 & 0 & 0 & 0 & 0 & -0.5454+\omega & 0.9508 & 0 & 0 & 0 & 0 \\ 0 & 0 & 0 & 0 & 0 & 0.9508 & 0.9508 & j & 0 & 0 & 0 \end{bmatrix}$$

Next, the submatrices representing the coupled resonators need to be evaluated. In this case, the coupling matrix that describes the behavior

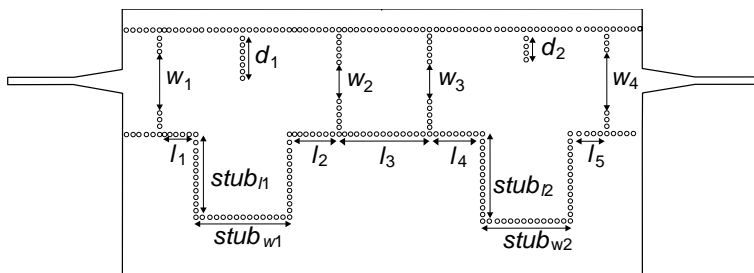


Figure 8. The layout of the fifth-order SIW *H*-plane filter.

of the subcircuit composed of coupled resonators 1 and 2 is obtained by deleting the fifth to the seventh column and row of the coupling matrix  $\mathbf{Z}$ . As a result, the matrix  $\mathbf{Z}^{12}$  is obtained.

$$\mathbf{Z}^{12} = \begin{bmatrix} 0 & 0.8455 & 0 & 0 \\ 0.8455 & -0.8417 + \omega & -0.9191 + 0.5527\omega & 0 \\ 0 & -0.9191 + 0.5527\omega & -0.4770 + \omega & 0.2340 \\ 0 & 0 & 0.2340 & 0 \end{bmatrix}.$$

The value of the external couplings between resonators 2 and 3 was computed using Eq. (11). The matrix representing the coupled resonators 4 and 5 was obtained in a similar way. The first three columns and rows of the matrix  $\mathbf{Z}$  were deleted, to give matrix  $\mathbf{Z}^{45}$

$$\mathbf{Z}^{45} = \begin{bmatrix} 0 & 0.2554 & 0 & 0 \\ 0.2554 & -0.2724 + \omega & -0.8811 + 0.3486\omega & 0 \\ 0 & -0.8811 + 0.3486\omega & -0.5454 + \omega & 0.9508 \\ 0 & 0 & 0.9508 & 0 \end{bmatrix}.$$

The reference zeros and poles for the first coupled pair are as follows:

$$\begin{aligned} rE_{12} &= [-0.7804 - 0.4792i, -0.3277 + 0.9153i] \\ rF_{12} &= [-0.3096 + 0.8744i, -0.6408 - 0.4383i] \\ rP_{12} &= [1.6630i]. \end{aligned}$$

For the fourth and fifth coupled resonators, the reference values of zeros and poles are as follows:

$$\begin{aligned} rE_{45} &= [-0.6870 - 0.5978i, -0.4164 + 0.8293i] \\ rF_{45} &= [0.3802 + 0.7809i, 0.5746 - 0.5494i] \\ rP_{45} &= [2.5274i] \end{aligned}$$

The final step is the dimensional synthesis. In this example, the direct couplings are implemented as inductive  $H$ -plane irises, while the dispersive couplings are implemented as shorted stubs with vertical septa. A comparison between the simulated and the ideal scattering parameters of the coupled pairs of resonators 1–2, 4–5 is presented in Figures 9 and 10 respectively. After a few iterations, a satisfactory result was achieved.

The final thing to do is to determine the length of the third resonator loaded by the second and the third coupling iris. This can be done as in Cohn's synthesis. When the widths of the loading irises are known, a corresponding reflection phase may be calculated. Next, this phase is incorporated in the calculation of the resonant length, as in [13].

The initial filter response once the synthesized resonators have been assembled is presented in Figure 11. It can be seen that the filter

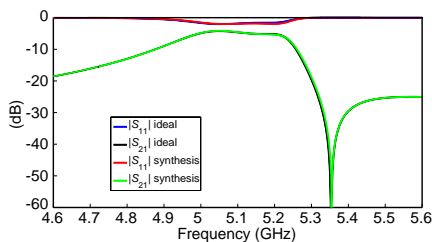


**Figure 9.** Synthesis of dispersive coupling between first and second resonators.

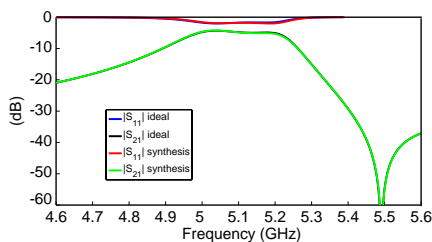


**Figure 10.** Synthesis of dispersive coupling between fourth and fifth resonators.

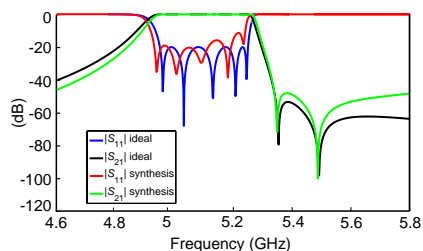


**Figure 11.** Simulated characteristics obtained after synthesis and ideal filter response.

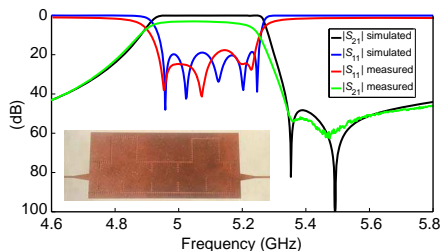


**Figure 12.** Simulated and measured fifth-order filter responses.

passband, as well as the return loss level, are nearly as expected. The return loss performance is degraded to approximately 16 dB at worst. Both transmission zeros are at the desired frequencies. The final tuning was made in Ansoft HFSS v.13 using a zero-pole goal function [21]. Only one iteration was needed to achieve a good result. A comparison between the dimensions obtained from the synthesis and the results of the final optimization is presented in Table 2. A comparison between the measured component and the ideal characteristics is shown in Figure 12. The filter bandwidth and the center frequency are nearly as designed. As can be seen, the filter return loss performance has been degraded to approximately 17.5 dB, which is a satisfactory result. The transmission characteristics show two transmission zeros in the upper stopband. The second of these is in the noise level, which is why it is not as clearly visible as the first one. The level of in-band insertion loss is approximately equal to 3 dB, and may be caused by the effect of losses, including those associated with the dielectric substrate, the finite conductivity of the top and bottom metalization layers, and the low quality of the metalization of the via holes.

**Table 2.** Dimensions for the  $H$ -plane substrate-integrated waveguide filter with quasielliptic characteristics.

$(Parameter)$	$(x_{synthesis})$	$(x_{optimization})$	$(Parameter)$	$(x_{synthesis})$	$(x_{optimization})$
$l_1$	5.7198	8.1537	$w_4$	13.9027	14.2683
$l_2$	8.3741	11.2183	$stub_{l_1}$	25.1000	18.7145
$l_3$	20.4400	20.4395	$stub_{l_2}$	21.4471	19.7149
$l_4$	10.6620	11.9188	$stub_{w_1}$	15.9396	21.1481
$l_5$	7.5302	8.2740	$stub_{w_2}$	16.8034	19.8094
$w_1$	13.5271	13.8560	$d_1$	9.3672	10.9097
$w_2$	8.7067	8.7993	$d_2$	5.5932	6.8697
$w_3$	8.9593	9.0152			

## 4. CONCLUSIONS

In this paper, a novel synthesis technique for coupled-resonator bandpass filters with frequency-dependent couplings has been proposed and validated. The method is based on the synthesis of two coupled resonators connected through a dispersive inverter, achieved by matching zeros and poles with the generalized eigenvalues of suitably defined matrix pencils, and taking into account loading effects resulting from external couplings.

## ACKNOWLEDGMENT

This work was supported by the National Science Centre under contract DEC-2011/01/B/ST7/06634.

## REFERENCES

1. Xu, Z., J. Guo, C. Qian, and W.-B. Dou, "A novel quasi-elliptic waveguide transmit reject filter for Ku-band VSAT transceivers," *Progress In Electromagnetics Research*, Vol. 117, 393–407, 2011.
2. Kuo, J.-T., S.-C. Tang, and S.-H. Lin, "Quasi-elliptic function bandpass filter with upper stopband extension and high rejection level using cross-coupled stepped-impedance resonators," *Progress In Electromagnetics Research*, Vol. 114, 395–405, 2011.
3. Cameron, R. J., "Advanced coupling matrix synthesis techniques for microwave filters," *IEEE Transactions on Microwave Theory and Techniques*, Vol. 51, No. 1, 1–10, 2003.

4. Lamecki, A., P. Kozakowski, and M. Mrozowski, "Fast synthesis of coupled-resonator filters," *IEEE Microwave and Wireless Components Letters*, Vol. 14, 174–176, 2004.
5. Kozakowski, P., A. Lamecki, P. Sypek, and M. Mrozowski, "Eigenvalue approach to synthesis of prototype filters with source/load coupling," *IEEE Microwave and Wireless Components Letters*, Vol. 15, 98–100, 2005.
6. Amari, S. and J. Bornemann, "Using frequency-dependent coupling to generate finite attenuation poles in direct-coupled resonator bandpass filters," *IEEE Microwave and Guided Wave Letters*, Vol. 9, No. 19, 404–406, 1999.
7. Amari, S., J. Bornemann, W. Menzel, and F. Alessandri, "Diplexer design using pre-synthesized waveguide filters with strongly dispersive inverters," *2001 IEEE MTT-S International Microwave Symposium Digest*, Vol. 3, 1627–1630, 2001.
8. Lamecki, A., P. Kozakowski, and M. Mrozowski, "Efficient implementation of the Cauchy method for automated CAD model construction," *IEEE Microwave and Wireless Components Letters*, Vol. 13, No. 7, 268–270, 2003.
9. Dziekonski, A., A. Lamecki, and M. Mrozowski, "GPU acceleration of multilevel solvers for analysis of microwave components with finite element method," *IEEE Microwave and Wireless Components Letters*, Vol. 21, No. 1, 1–3, 2011.
10. Dziekonski, A., A. Lamecki, and M. Mrozowski, "A memory efficient and fast sparse matrix vector product on a GPU," *Progress In Electromagnetics Research*, Vol. 116, 49–63, 2011.
11. Dziekonski, A., A. Lamecki, and M. Mrozowski, "Tuning a hybrid GPU-CPU V-cycle multilevel preconditioner for solving large real and complex systems of FEM equations," *Antennas and Wireless Propagation Letters*, Vol. 10, 619–622, 2011.
12. Dziekonski, A., P. Sypek, A. Lamecki, and M. Mrozowski, "Finite element matrix generation on a GPU," *Progress In Electromagnetics Research*, Vol. 128, 249–265, 2012.
13. Matthaei, G. L., L. Young, and E. M. T. Jones, *Microwave Filters, Impedance-matching Networks and Coupling Structures*, Artech House, 1985.
14. Szydłowski, L., N. Leszczynska, A. Lamecki, and M. Mrozowski, "A substrate integrated waveguide (SIW) bandpass filter in a box configuration with frequency-dependent coupling," *IEEE Microwave and Wireless Components Letters*, Vol. 22, No. 11, 556–558, 2012.

15. Zhang, Q. L., W. Y. Yin, and S. He, "Evanescent-mode substrate integrated waveguide (SIW) filters implemented with complementary split ring resonators," *Progress In Electromagnetics Research*, Vol. 111, 419–432, 2011.
16. Wu, L. S., J. F. Mao, W. Shen, and W. Y. Yin, "Extended doublet bandpass filters implemented with microstrip resonator and full-/half-mode substrate integrated cavities," *Progress In Electromagnetics Research*, Vol. 108, 433–447, 2010.
17. Wang, Z. G., X. Q. Li, S. P. Zhou, B. Yan, R. M. Xu, and W. G. Lin, "Half mode substrate integrated folded waveguide (HMSIFW) and partial  $H$ -plane bandpass filter," *Progress In Electromagnetics Research*, Vol. 101, 203–216, 2010.
18. Szydlowski, L., A. Lamecki, and M. Mrozowski, "Design of microwave lossy filter based on substrate integrated waveguide (SIW)," *IEEE Microwave and Wireless Components Letters*, Vol. 21, No. 5, 249–251, May 2011.
19. Jedrzejewski, A., N. Leszczynska, L. Szydlowski, and M. Mrozowski, "Zero-pole approach to computer aided design of in-line SIW filters with transmission zeros," *Progress In Electromagnetics Research*, Vol. 131, 517–533, 2012.
20. Szydlowski, L., A. Lamecki, and M. Mrozowski, "Coupled-resonator filters with frequency-dependent couplings: Coupling matrix synthesis," *IEEE Microwave and Wireless Components Letters*, Vol. 22, No. 6, 312–314, 2012.
21. Kozakowski, P. and M. Mrozowski, "Automated CAD of coupled resonator filters," *IEEE Microwave and Wireless Components Letters*, Vol. 12, No. 12, 470–472, 2002.
22. Gustavsen, B. and A. Semlyen, "Rational approximation of frequency domain responses by vector fitting," *IEEE Transactions Magnetics*, Vol. 39, No. 6, 3581–3586, 2003.